crystals

MDPI

Article

Maximizing the Light Extraction Efficiency for AlGaN-Based DUV-LEDs with Two Optimally Designed Surface Structures under the Guidance of PSO

Zizheng Li [1], Huimin Lu [1,*], Jianping Wang [1], Yifan Zhu [1], Tongjun Yu [2] and Yucheng Tian [2]

1 School of Computer and Communication Engineering, University of Science and Technology Beijing, Beijing 100083, China
2 The State Key Laboratory for Mesoscopic Physics, School of Physics, Peking University, Beijing 100871, China
* Correspondence: hmlu@ustb.edu.cn

Abstract: A novel method of utilizing an intelligent algorithm to guide the light extraction surface structure designing process for deep-ultraviolet light emitting diodes (DUV-LEDs) is proposed and investigated. Two kinds of surface structures based on the truncated pyramid array (TPA) and truncated cone array (TCA) are applied, which are expected to suppress the total internal reflection (TIR) effect and increase the light extraction efficiency (LEE). By addressing particle swarm optimization (PSO), the TPA and TCA microstructures constructed on the sapphire layer of the flip-chip DUV-LEDs are optimized. Compared to the conventional structure design method of parameter sweeping, this algorithm has much higher design efficiency and better optical properties. At the DUV wavelength of 280 nm, as a result, significant increases of 221% and 257% on the LEE are realized over the two forms of optimized surface structures. This approach provides another design path for DUV-LED light extraction structures.

Keywords: DUV-LED; light extraction efficiency; particle swarm algorithm; microstructure optimization

check for updates

Citation: Li, Z.; Lu, H.; Wang, J.; Zhu, Y.; Yu, T.; Tian, Y. Maximizing the Light Extraction Efficiency for AlGaN-Based DUV-LEDs with Two Optimally Designed Surface Structures under the Guidance of PSO. *Crystals* **2022**, *12*, 1700. https://doi.org/10.3390/cryst12121700

Academic Editor: Dah-Shyang Tsai

Received: 25 October 2022
Accepted: 22 November 2022
Published: 24 November 2022

1. Introduction

AlGaN-based deep-ultraviolet light-emitting diodes (DUV-LEDs) have widely drawn attention from academia and industry for their promising potential in sanitation disinfection, medical diagnosis, microstructure lithography, confidential communication, the fight against coronavirus, and so on [1–4]. In spite of the numerous efforts by predecessors [5], the external quantum efficiency (EQE) of DUV-LEDs still remains extremely low, resulting in a much weaker output power compared with the common LEDs in other wavelength ranges. Two major causes of this are the high-density dislocation in epitaxial layers and the extremely low light extraction efficiency (LEE) [6,7]. Fabricating DUV-LEDs on the AlN substrate can overcome the dislocation problem, meanwhile enhancing the device's reliability. To avoid the high absorption of DUV light in the P-region, flip-chip configuration is widely used such that the light extraction process happens in the transparent sapphire layer. However, high refractive index contrast at the interface between the epitaxial layer and ambient medium induces total internal reflection (TIR) in a wide range of incidence angles, which can lead to a significant decline of the extracted light from the LEDs surface. It has been proved that at the wavelength of 280 nm, mostly TE [8]. Therefore, a range of studies on light extraction enhancement by using certain microstructures has been performed, including moth-eye structure array, cone array, nanoimprinted structures, and so on [9–13]. However, systematic optimization of such surface structures has not yet been reported.

Remarkable progress has been made by intelligent algorithms in the design process of photonic devices, for the structure optimization design is such an extremely time-consuming process that it requires enormous computing power if the conventional working flow, which relies on the human brain and experience along with exhaustive parameter sweeps, is adopted [14]. In general, the intelligent algorithm-driven design methods are firstly initialized by a rational precondition (obtained from human guess or experience) and iterate by calculating the performances then updating the parameters and photonic structure for multiple generations to satisfy the ultimate expectations [15–18]. Broadly speaking, intelligent algorithms that are addressed in device design include optimization algorithms (e.g., particle swarm optimization (PSO) and genetic algorithm (GA)), topological optimization (TO), and deep learning (DL) algorithms (e.g., generative adversarial network (GAN)). The design process of the three-dimensional devices addressing has been illustrated. For the task of designing a light extraction structure for DUV-LEDs that demands a huge amount of calculation time in one single simulation, along with multiple parameters linearly and non-linearly affecting the optical response that need to be determined, PSO is the most effective and accurate method in comparison with other intelligent algorithms. The traditional and most applied method, parameter sweep, searches every grid point in the grid net to find an optimal combination of parameters, which is certainly inefficient and not worthy when too many simulation runs are required. DL requires a large-scale dataset and is greatly dependent on the quality of the dataset. Besides, it could become inoperable to build such a dataset if each sample is obtained by a time-consuming FDTD simulation method. Apart from that, methods such as GA are low efficient for the slow convergence with the mutation and exchange procedure. Both of them provide strong resistance to being trapped in local optimum, which overkill the tasks with some number of parameters to determine, such as the one here for DUV-LEDs.

In this work, we propose a novel design scheme for the light extraction surface structures of AlGaN-based DUV-LEDs. By modifying the structural parameters under the guidance of an intelligent algorithm, we maximize the LEE. On this basis, two kinds of light extraction surface microstructures, a truncated pyramid array and a truncated cone array, are applied and optimized. The basic theory and properties of the microstructures are discussed first. Then, the parameter optimization trends and the changes in optical responses during the algorithm iterations are identified using three-dimensional (3D) finite difference time domain (FDTD) simulations. Finally, compared with the conventional flat sapphire surface, the superior optical properties contributed from the optimized surface structures using the proposed design scheme are analyzed and discussed for DUV-LEDs.

2. Methods

The perspective view of the two kinds of adopted surface structures is given in Figure 1, which is expected to improve the DUV-LEDs LEE through theoretical prediction. As shown in Figure 1, in order to minimize TIR, two light extraction surface structures, truncated pyramid array (TPA) and truncated cone array (TCA), are applied to be planted at the interface of sapphire and air. The thickness of the sapphire base (substrate under TPA and TCA), AlN layer, and the n-AlGaN layer are 2 μm, 1 μm, and 2 μm, respectively. Below them, there are multiple-quantum-well (MQW) layers, p-AlGaN layers, and p-GaN layers (shown in the subgraph), all of which the thickness is 0.1 μm. The side lengths of the top and bottom sides of the truncated pyramid are d_1 and d_2, while the radii of that in truncated cone are marked as r_1 and r_2, respectively. Parameter hp and hc represent the height of the TPA and TCA. The refractive indexes of the sapphire, AlN, n-AlGaN, MQW, p-AlGaN, and p-GaN are 1.823, 2.16, 2.6, 2.7, 2.6, and 2.9, respectively. Additionally, the absorption coefficients of the AlGaN, MQW, and GaN are set to 170,000 cm^{-1}, 1000 cm^{-1}, and 10 cm^{-1} [10], respectively. It is assumed that the absorption induced by sapphire and AlN layers can be ignored. At the sapphire-air interface, there is a huge refractive index change of 0.823, which can cause that any light injected with an incident angle bigger than 33° will be reflected back to the sapphire medium. We introduced the TPA and TCA surface structures to guide this part of light into the periodical microstructures, that way it can propagate into air directly or after a couple of times of reflection.

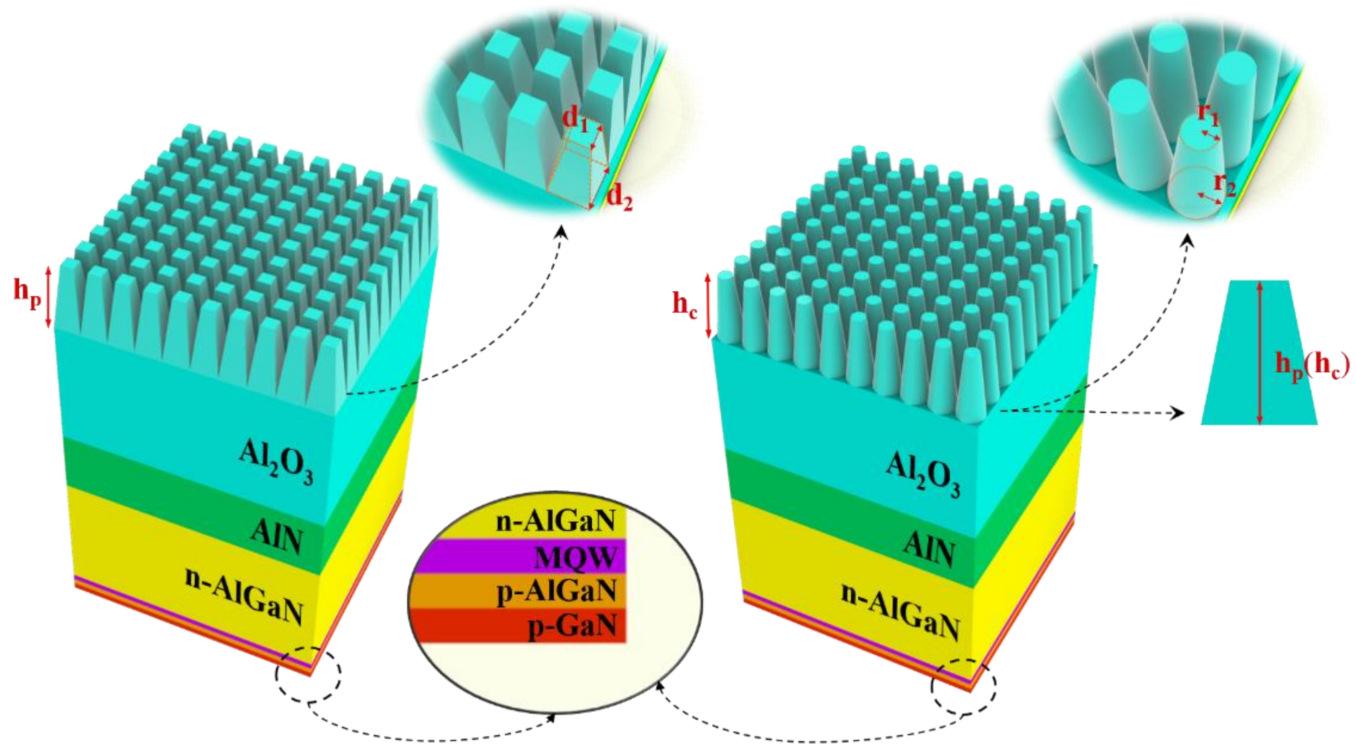

Figure 1. Perspective view of truncated-pyramid surface and truncated-cone surface DUV-LEDs.

In this work, the intelligent algorithm of PSO is utilized to search for the optimal parameter solution set of the surface microstructures, in order to gain the highest DUV-LEDs LEE. First, the microstructures are digitalized into three sets of structural parameters, height h, top scale d_1, r_1, bottom scale d_2, r_2. These parameters uniquely determine the structure of the TPA and TCA, given that the truncated pyramids and cones abut on each other. The parameter space is expressed by particles in PSO and the swarm consists of m particles as follows: S = {X_1, X_2, . . . , X_m}, where each particle is an n-dimensional vector as follows: X_m = {$x_{m,1}$, $x_{m,2}$, . . . , $x_{m,n}$}. Here, the number of particles is set to m = 6, which can lessen redundant computation and reduce time consumption. The particle dimension indicates the parameter space. Therefore, n = 3 and the vector for TPA is $x_{m,n}$ = {d_1, d_2, h} while for TPC is $x_{m,n}$ = {r_1, r_2, h}. Before running the PSO, the particles are randomly located in predetermined range and given random altering velocities [15]. Limited by the material growth in experiment, parameter h is preset within the range of [0 μm, 5 μm], and bottom scale parameters d_2, r_2 within the range of [0 μm, 1 μm]. The top scale parameters d_1, r_1 are set to values that are always not bigger than d_2 and r_2 respectively, ensuring keep in the shape of truncated pyramid and truncated cone. The figure of merits (FOM) is defined as the total power extracted from the LED at wavelength 280 nm. Therefore, the overall goal is to find the optimal solution that maximum the FOM. During the PSO iterative process, the particle location and velocity are updated by Equations (1) and (2) as follows:

$$x_{m,n} = x_{m,n} + v_{m,n} \tag{1}$$

$$v_{m,n} = \omega \times v_{m,n} + c_1 \times rand \times (p_{best,mn} - x_{m,n}) + c_2 \times rand \times (g_{best,mn} - x_{m,n}) \tag{2}$$

where $p_{best,mn}$ is the individual best position of the particle and $g_{best,mn}$ is the global best position of the swarm. Additionally, inertial weight ω determines the intention of the particle that prefers to keep the old velocity. The cognitive rate and social rate, c_1 and c_2, are to adjust the influence of individual and global best solutions. The random number *rand* is uniformly distributed in the range of [0, 1]. The PSO process ends when either of the following two terminating conditions are satisfied: 1. FOM shows no change in the last generations; 2. PSO hit the maximum generation number.

The 3D-FDTD algorithm is applied to perform the FOM calculation in each PSO iteration. A single dipole source, of which the wavelength and line width are 280 nm and 10 nm respectively, is placed at the center of the MQW region. Note that the TM mode is ignored in DUV-LEDs around the wavelength of 280 nm [8]. Therefore, the dipole source is polarized in the direction that is parallel to the MQW plane to only excite the TE mode. It is known that 3D-FDTD simulation meets great difficulty in large structures that exceed the scale of a hundred times of wavelength. To avoid too much time consuming, we limit the horizontal scale of the simulated region to approximately 4 μm × 4 μm. It is much smaller than the actual LED size, though still can reflect the real situation by covering the perfect electrical conductor (PEC) blocks on lateral sides of simulated region, which are acting as perfect mirrors that stop any power escaping laterally [19–21]. The extracted power is detected by the monitor at the top of the simulation region. The LEE is calculated in terms of the power extracted from the top side of the LED divided by the source power.

3. Results

In this work, two forms of light extraction microstructures, TPA and TCA, are analyzed and optimized by PSO at the sapphire-air interface, separately, in order to maximize the LEE of AlGaN-based DUV-LEDs. There are 6 particles in both tasks, marked as a, b, c, d, e, and f. Figure 2a,b gives the updated trends of the particles in the PSO progress for the two surface microstructures. It takes 12 generations of PSO iterations to find the optimal solution for the TPA structure, as shown in Figure 2a, while two more generations are taken for the TCA, shown in Figure 2b. These two sub-figures share the same color bar that indicates the specific LEE of a certain particle in a certain generation. In the first generation of PSO, the structural parameters are preset as the circumstance that there is no light extraction structure, and they are allocated with a random updating velocity. Particles then vary to find the individual best position in each generation and eventually gather at the global best position. The preset maximum generation numbers for the two tasks are both 20. However, neither of them hits it, and they both terminated by the terminating condition of no raise on FOM for the last three generations. It is worth to be noted that the preset conditions play a crucial part in the PSO procedure. We tested that if the number of particles is smaller than five, they may fall into a local maximum and find it difficult to jump out, and the PSO will not be terminated even after 20 generations. That leads to wrong solutions and time wasting. Nevertheless, drawing too many particles can reach the right solution but can also be time-consuming because the total time spent is the product of the number of particles, the number of generations, and the time of a single 3D-FDTD simulation.

In Figure 2c, the LEE varying trends over the PSO generations for the AlGaN-based DUV LED with the two surface microstructures are given and compared with that for the conventional LED. The yellow line labeled "Convention" represents a conventional LED without any light extraction structure. As for the TPA and TCA, in the first two generations, the search range is rapidly narrowed down, where the LEE has reached more than 10%. In the generations of 3~10, there are steadily minor increases in LEE. After generation 10, the changes in LEE become so small that eventually, the PSO is stopped by the first terminating condition. The values of $p_{best,mn}$ and $g_{best,mn}$ are updated during this procedure after each generation, and finally, the FOM reaches its maximum. It is worth mentioning that the LEEs obtained in the 13th and 14th generations are not included in Figure 2c because the LEE value in the last 3 generations remains the same. In comparison, the final optimal LEE of the LED with TPA is higher than that of the TCA because TPA can cover the entire sapphire-air interface more densely so that the light propagating through the sapphire layer will be fully guided into the microstructures. A 221% increment for TCA and a 257% increment for TPA are realized when compared to conventional LED.

The updating trends of the structural parameters for the two surface microstructures are also analyzed and given in Figure 3, which records the value of each parameter at the end of every generation in the PSO process. Figure 3a,b show the three parameters {d_1, d_2, h}, and it contains {r_1, r_2, h} for TPA and TCA microstructure, respectively. Solid lines corresponding to the left *y*-axis are applied to the side length and diameter, while the dashed line corresponding to the right *y*-axis is applied to the height. As shown in Figure 3, the optimal solution obtained by the PSO is {d_1, d_2, h} = {0.31, 0.13, 5}, and {r_1, r_2, h} = {0.58, 0.19, 5}. In both cases for the TPA and TCA, the height h has been optimized to the preset range maximum value of 5 µm, suggesting that the height is a linear impact factor to the LEE. Actually, the higher the pyramids and cones are, the bigger the LEE. Additionally, if the microstructures can be extended upward infinitely, there will no longer be any TIR and the LEE encounters no decay. The parameters of side length and diameter show nonlinearity, and they fluctuate through the whole process with gradually decreasing amplitude. Finally, when the PSO is terminated, all the parameters tend to be stationary.

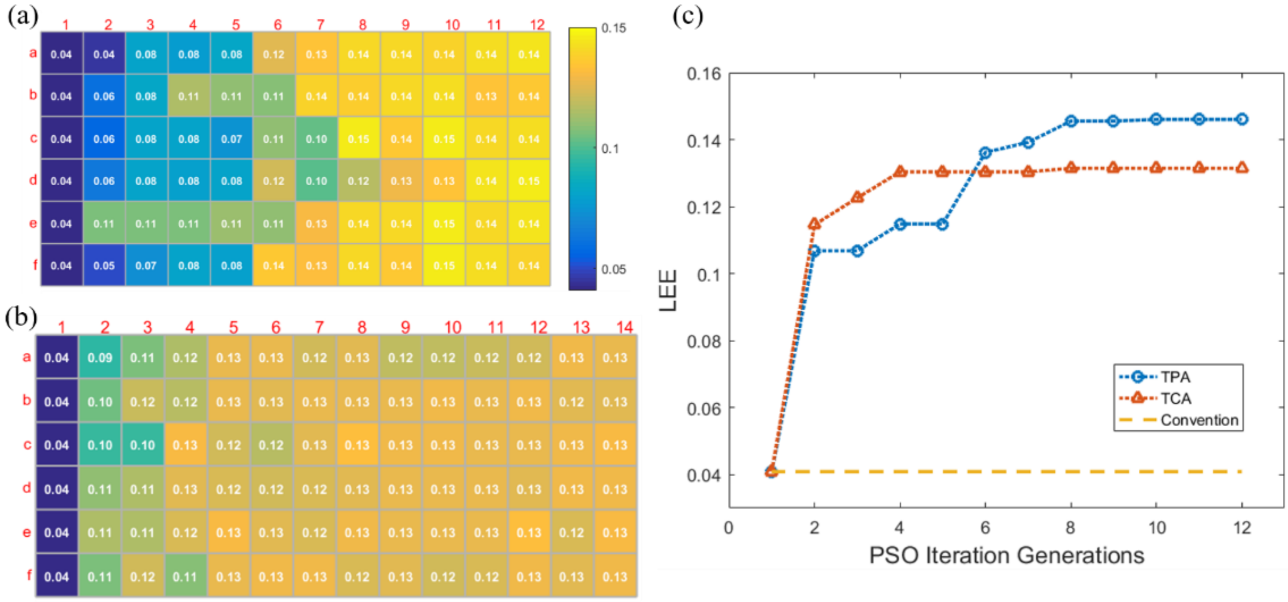

Figure 2. Updating trends of the particles in the structure of (**a**) the TPA and (**b**) the TCA, and (**c**) the comparison on the LEE enhancement trends.

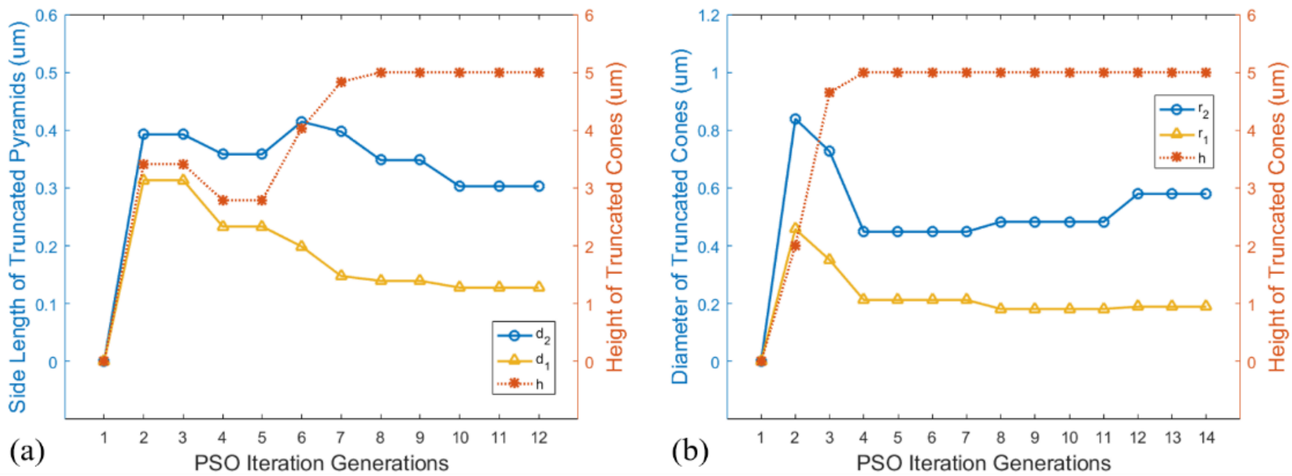

Figure 3. Updating trends of the structural parameters in (**a**) the TPA and (**b**) the TCA.

In this work, the task of determining structural parameters in TPA and TCA can be abstracted as finding the maximum of the function of multiple variables. The nonlinear relationship between the parameters and the LEE and the time-consuming FDTD calculations are the notable difficulty. The advantages of the PSO algorithm are highlighted in this procedure since there is no necessity to draw support from parameter sweeps or enumeration attempts. Suppose that we use the conventional method of parameter sweeping to determine such a structure with multiple parameters; even though they are independent of each other, we still have to split the whole task and spend a lot of time to find out how each parameter affects the LEE. This process deals with the parameters separately, it works only if the effect of the parameters on the FOM is linear, but it becomes hard to tell the way they affect the LEE jointly. In that case, all sorts of combinations of certain parameters need to be enumerated, and every time, a 3D-FDTD simulation is needed. However, with just a complete PSO procedure, the optimal values of all the parameters of a microstructure can be determined, greatly reducing the number of runs of FDTD simulations.

The optical field distribution for the AlGaN-based DUV-LEDs with the optimized surface microstructure is further investigated and compared with the conventional LEDs. The cross-sectional field distributions and light power variation trend in the direction horizontal to the MQW plane are shown in Figure 4. In the light extraction process, the biggest LEE decrease happens at the interface between the MQW layer and the n-AlGaN layer. More than half of the source power has been trapped in the MQW layer due to the high absorption and TIR at the interface. As depicted in Figure 4a, in the n-AlGaN layer and AlN layer, relatively low absorption occurs. Apart from the one near the dipole source, interfaces between every two adjoint layers cause TIR, which turns out to be the primary negative impact on light extraction. At the Al2O3-air interface, the normalized powers (which are actually the LEEs) influenced by three kinds of structures (no structure, TPA, and TCA) are compared. It can be seen that without any light extraction structures, the LEE of LED can finally be significantly low, even smaller than 5%. The TPA and TCA make it to raise the LEEs higher than 14.6% and 13.1%. In Figure 4b,c, the field distributions of the cross-section that is perpendicular to the MQW plane are illustrated. The white short, dashed lines are applied to highlight the boundaries of each layer. The power decrease in the light while propagating is shown in a more clear and visualized way. In the last part of the journey, where the effect of the TPA and TCA is highlighted. With proper structural parameters optimized by the PSO, the light propagates into the truncated pyramid or truncated cone microstructures in different directions, suffering little from TIR, then is refracted from sapphire into the air directly or after several reflections.

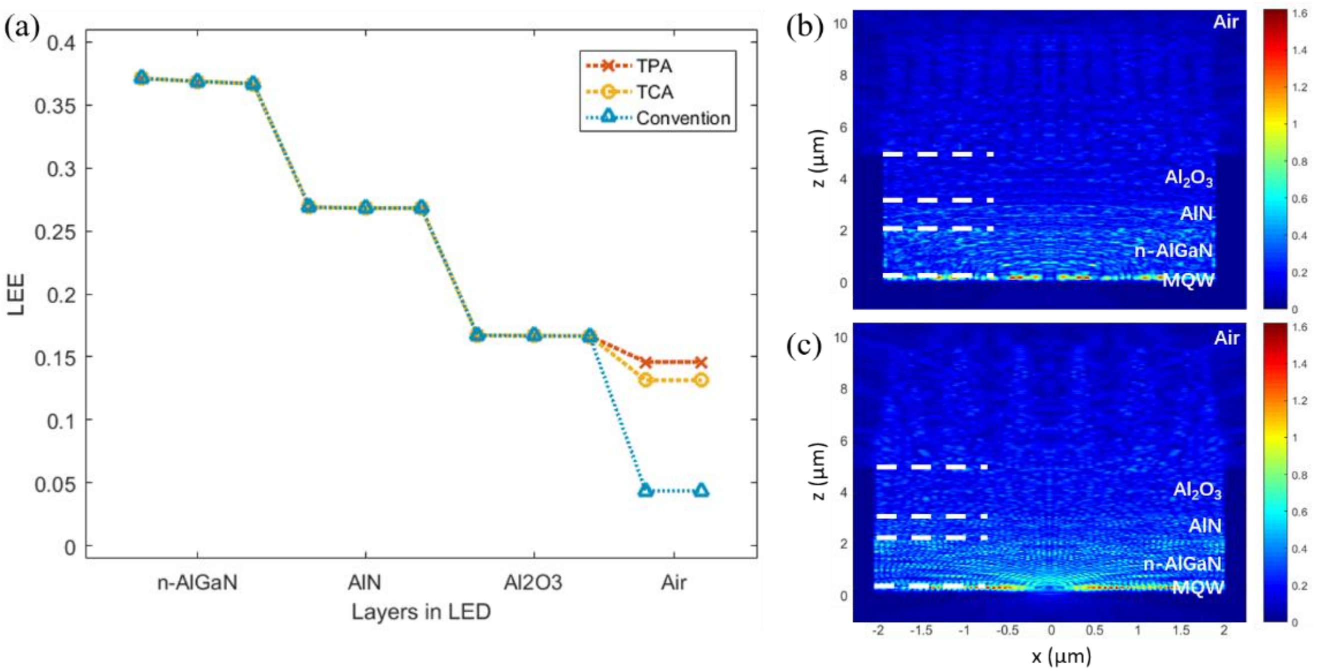

Figure 4. (**a**) The comparison of LEE decrement trends along LED layers, and the field distributions in the LED cross section with (**b**) TPA and (**c**) TCA.

The far-field scattering angular distribution for a specified wavelength of 280 nm is shown in Figure 5. It is calculated outside of a box-like closed surface constructed by monitors placed in homogeneous material by 3D-FDTD, according to the surface equivalence theory. Identical settings are taken to simulate the far-field distributions of the LEDs with TPA and TCA. In the conventional LED, without any light extraction structures, the main energy of the extracted light is located within the angle range (60°, 120°) owing to the TIR at the sapphire–air interface. There is still a small amount of light extracted from other angles. It is noticed that the intensity of the extracted light is largely increased with the surface structure of TPA or TCA. With the TCA, the extracted light intensity has been increased by ~1.5 folds at (75°, 115°), and ~2 folds at all other angles. With TPA, the extracted light at (75°, 115°) is less than that with TCA, but it extracts much more light at other angles, and the total power extracted by TPA is 11% more than that by TCA. There are no gaps or lacunas in the base of the TPA, which brings about collecting light at a larger angle range and larger LEE. However, above that, the four flat side walls in the truncated pyramid microstructures can cause more TIR than the truncated cone microstructure, which limits the amount of light extracted at (75°, 115°).

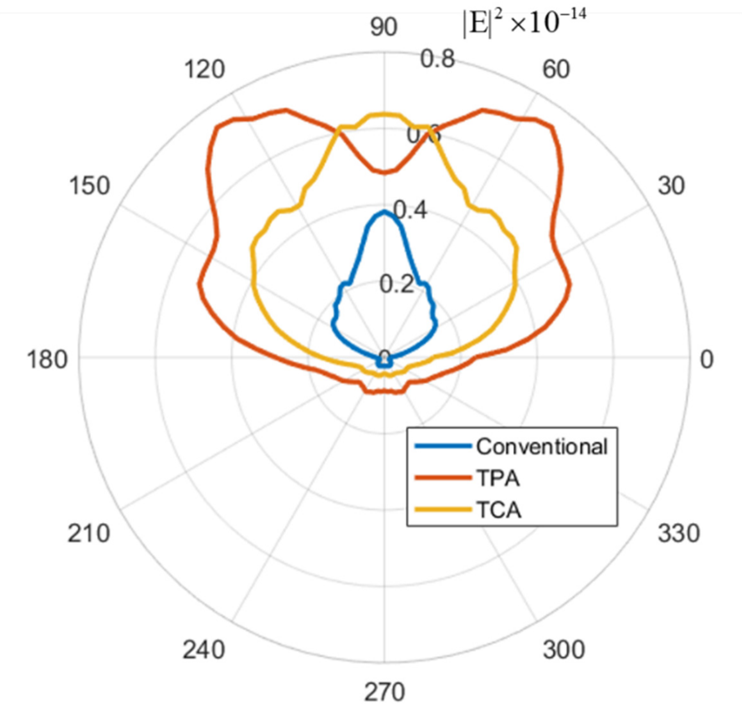

Figure 5. Far-field distribution of the LEDs with three structures.

This work is focused on the LEE enhancement in DUV-LEDs with TPA and TCA. With the help of an intelligent algorithm, we have met a clear enhancement in the LEE. Nevertheless, neither the TPA nor TCA may not be the best option for light extraction; more forms of microstructures, not only the ones located on the sapphire-air surface, can be designed and tested with the same method. The number of parameters can be expanded in order to represent more complicated microstructures.

4. Conclusions

In summary, maximizing the LEE has been the major goal for the AlGaN-based DUV-LEDs design. Here, we propose a novel scheme to cope with the main difficulty in the optimal design process as follows: consuming too much time in a parametric sweep. Drawing help from the intelligent algorithm PSO, the number of simulations in this work has been significantly reduced, and the whole process has become much more efficient. As a result, with the light extraction structures TPA and TCA, a 221% and a 257% LEE enhancement are realized at the DUV wavelength of 280 nm when compared to the conventional LEDs. The 3D-FDTD method is utilized to verify the optical properties. This method shows advantages in designing tasks that contain multiple parameters nonlinearly affecting the goal in DUV-LEDs, and it is expected to provide a new path for LED device design.

Author Contributions: Conceptualization, H.L. and T.Y.; methodology, Z.L., Y.Z. and Y.T.; software, Z.L.; validation, Z.L., Y.Z. and Y.T.; formal analysis, Z.L.; investigation, Y.Z.; resources, H.L., J.W. and T.Y.; data curation, Z.L. and Y.Z.; writing—original draft preparation, Z.L.; writing—review and editing, Y.Z., H.L. and J.W.; visualization, Z.L.; supervision, H.L. and J.W.; project administration, H.L.; funding acquisition, H.L. All authors have read and agreed to the published version of the manuscript.

Funding: This research was funded by the Guangdong Basic and Applied Basic Research Foundation, grant number 2021B1515120086; the Scientific and Technological Innovation Foundation of Foshan, grant number BK20BF013.

Data Availability Statement: The data presented in this study are available on request from the corresponding author.

Conflicts of Interest: The authors declare no conflict of interest.

References

1. Khan, A.; Balakrishnan, K.; Katona, T. Ultraviolet Light-Emitting Diodes Based on Group Three Nitrides. *Nat. Photonics* **2008**, *2*, 77–84. [CrossRef]
2. Kneissl, M.; Kolbe, T.; Chua, C.; Kueller, V.; Lobo, N.; Stellmach, J.; Knauer, A.; Rodriguez, H.; Einfeldt, S.; Yang, Z.; et al. Advances in Group III-Nitride-Based Deep UV Light-Emitting Diode Technology. *Semicond. Sci. Technol.* **2011**, *26*, 014036. [CrossRef]
3. Vilhunen, S.; Särkkä, H.; Sillanpää, M. Ultraviolet Light-Emitting Diodes in Water Disinfection. *Environ. Sci. Pollut. Res.* **2009**, *16*, 439–442. [CrossRef] [PubMed]
4. Li, J.; Gao, N.; Cai, D.; Lin, W.; Huang, K.; Li, S.; Kang, J. Multiple Fields Manipulation on Nitride Material Structures in Ultraviolet Light-Emitting Diodes. *Light Sci. Appl.* **2021**, *10*, 129. [CrossRef]
5. Guo, Y.; Yan, J.; Zhang, Y.; Wang, J.; Li, J. Enhancing the Light Extraction of AlGaN-Based Ultraviolet Light-Emitting Diodes in the Nanoscale. *J. Nanophoton.* **2018**, *12*, 043510. [CrossRef]
6. Du, P.; Zhang, Y.; Rao, L.; Liu, Y.; Cheng, Z. Enhancing the Light Extraction Efficiency of AlGaN LED with Nanowire Photonic Crystal and Graphene Transparent Electrode. *Superlattices Microstruct.* **2019**, *133*, 106216. [CrossRef]
7. Du, P.; Cheng, Z. Enhancing Light Extraction Efficiency of Vertical Emission of AlGaN Nanowire Light Emitting Diodes With Photonic Crystal. *IEEE Photonics J.* **2019**, *11*, 1600109. [CrossRef]
8. Wang, H.; Fu, L.; Lu, H.M.; Kang, X.N.; Wu, J.J.; Xu, F.J.; Yu, T.J. Anisotropic Dependence of Light Extraction Behavior on Propagation Path in AlGaN-Based Deep-Ultraviolet Light-Emitting Diodes. *Opt. Express* **2019**, *27*, A436. [CrossRef]
9. Wang, S.; Dai, J.; Hu, J.; Zhang, S.; Xu, L.; Long, H.; Chen, J.; Wan, Q.; Kuo, H.; Chen, C. Ultrahigh Degree of Optical Polarization above 80% in AlGaN-Based Deep-Ultraviolet LED with Moth-Eye Microstructure. *ACS Photonics* **2018**, *5*, 3534–3540. [CrossRef]
10. Ryu, H.-Y.; Choi, I.-G.; Choi, H.-S.; Shim, J.-I. Investigation of Light Extraction Efficiency in AlGaN Deep-Ultraviolet Light-Emitting Diodes. *Appl. Phys. Express* **2013**, *6*, 062101. [CrossRef]
11. Zhang, G.; Shao, H.; Zhang, M.; Zhao, Z.; Chu, C.; Tian, K.; Fan, C.; Zhang, Y.; Zhang, Z.-H. Enhancing the Light Extraction Efficiency for AlGaN-Based DUV LEDs with a Laterally over-Etched p-GaN Layer at the Top of Truncated Cones. *Opt. Express* **2021**, *29*, 30532. [CrossRef] [PubMed]
12. Sun, W.C.; Hsu, B.; Wei, M.K. Micro-Truncated Cone Arrays for Light Extraction of Organic Light-Emitting Diodes. In *TMS 2016 145th Annual Meeting & Exhibition*; Springer: Cham, Switzerland, 2016; pp. 473–479. [CrossRef]
13. Inoue, S.; Tamari, N.; Taniguchi, M. 150 MW Deep-Ultraviolet Light-Emitting Diodes with Large-Area AlN Nanophotonic Light-Extraction Structure Emitting at 265 Nm. *Appl. Phys. Lett.* **2017**, *110*, 141106. [CrossRef]
14. Wang, N.; Yan, W.; Qu, Y.; Ma, S.; Li, S.Z.; Qiu, M. Intelligent Designs in Nanophotonics: From Optimization towards Inverse Creation. *PhotoniX* **2021**, *2*, 22. [CrossRef]
15. Zhang, Y.; Yang, S.; Lim, A.E.-J.; Lo, G.-Q.; Galland, C.; Baehr-Jones, T.; Hochberg, M. A Compact and Low Loss Y-Junction for Submicron Silicon Waveguide. *Opt. Express* **2013**, *21*, 1310. [CrossRef]
16. Forestiere, C.; Donelli, M.; Walsh, G.F.; Zeni, E.; Miano, G.; Dal Negro, L. Particle-Swarm Optimization of Broadband Nanoplasmonic Arrays. *Opt. Lett.* **2010**, *35*, 133. [CrossRef] [PubMed]
17. Zhang, B.; Chen, W.; Wang, P.; Dai, S.; Li, H.; Lu, H.; Ding, J.; Li, J.; Li, Y.; Fu, Q.; et al. Particle Swarm Optimized Polarization Beam Splitter Using Metasurface-Assisted Silicon Nitride Y-Junction for Mid-Infrared Wavelengths. *Opt. Commun.* **2019**, *451*, 186–191. [CrossRef]
18. Shokooh-Saremi, M.; Magnusson, R. Particle Swarm Optimization and Its Application to the Design of Diffraction Grating Filters. *Opt. Lett.* **2007**, *32*, 894. [CrossRef]

19. Ryu, H.Y. Numerical Study on the Wavelength-Dependence of Light Extraction Efficiency in AlGaN-Based Ultraviolet Light-Emitting Diodes. *Opt. Quant. Electron.* **2014**, *46*, 1329–1335. [CrossRef]
20. Ryu, H.Y.; Shim, J.-I. Structural Parameter Dependence of Light Extraction Efficiency in Photonic Crystal InGaN Vertical Light-Emitting Diode Structures. *IEEE J. Quantum Electron.* **2010**, *46*, 714–720. [CrossRef]
21. Zhao, P.; Zhao, H. Analysis of Light Extraction Efficiency Enhancement for Thin-Film-Flip-Chip InGaN Quantum Wells Light-Emitting Diodes with GaN Micro-Domes. *Opt. Express* **2012**, *20*, A765. [CrossRef]